# Gas-Phase Reaction of Hydrated $CO_2^{\bullet-}$ Anion Radical with $CH_3I$

**Tatsuya Tsukuda[†] and Takashi Nagata*[,‡]**

*Institute for Molecular Science, Myodaiji, Okazaki 444-8585, Japan, and the Department of Basic Science, Graduate School of Arts and Sciences, The University of Tokyo, Komaba, Meguro-ku, Tokyo 153-8902, Japan*

*Received: April 22, 2003*

Hydrated $CO_2^{\bullet-}$ anion radicals, $CO_2^{\bullet-}(H_2O)_N$, are selectively prepared in an electron-impact free jet of $CO_2$ containing $H_2O$. Mass spectrometric measurement reveals that $CO_2^{\bullet-}(H_2O)_N$ reacts with $CH_3I$ to form an anion with $[(CO_2)(CH_3I)]^-$ stoichiometry. The product $[(CO_2)(CH_3I)]^-$ is further identified as the anion of acetyloxy iodide, $CH_3CO_2I^-$, based on the observation that $[(CO_2)(CH_3I)]^-$ photodissociates at 532 nm into $CH_3CO_2^-$ + I or $CH_3CO_2$ + $I^-$ channels. The $CO_2^{\bullet-}(H_2O)_N$ + $CH_3I$ reaction thus presents a sharp contrast to the corresponding reaction in solutions: the gas-phase $CO_2^{\bullet-}(H_2O)_N$ behaves as a carboxylation reagent for alkyl halides (RX), whereas in aqueous solutions the reaction proceeds as $CO_2^{\bullet-}$ + RX → $CO_2$ + R + $X^-$. Ab intio calculations suggest that $CO_2^{\bullet-}(H_2O)_N$ can take on structures preferable for radical reactions: the hydration occurs on the O atoms of $CO_2^{\bullet-}$ and the unpaired electron on the C atom remains uncovered with $H_2O$ solvents. The reaction mechanism of the $CO_2^{\bullet-}(H_2O)_N$ + $CH_3I$ process is discussed in conjunction with previous results of $(CO_2)_N^-$ + $CH_3I$ studies (*J. Phys. Chem.* **1997**, *A101*, 5103).

## Introduction

The chemistry of carbon dioxide anion radical, $CO_2^{\bullet-}$, continues to receive much attention from the viewpoint of chemical activation and utilization of stubbornly inert carbon dioxide.[1,2] In aqueous chemistry, $CO_2^{\bullet-}$ usually acts as a one-electron reducing agent for many kinds of organic compounds.[3−6] Nucleophilic addition reactions of $CO_2^{\bullet-}$ have also been reported,[7,8] indicating the dual reactivity of $CO_2^{\bullet-}$ as a radical and/or anionic reagent. These investigations have proved the transformation into $CO_2^{\bullet-}$ to be the effective means for activating $CO_2$. It is, however, also revealed that the negative electron affinity of $CO_2$ eventually gives rise to a difficulty in the direct reductive activation of $CO_2$. One of the applicable ways to form $CO_2^{\bullet-}$ in aqueous media is the reaction of hydroxyl or sulfate radicals with formate ions:[3,8]

$$OH^{\bullet} + HCO_2^- \rightarrow CO_2^{\bullet-} + H_2O \qquad (1a)$$

$$SO_4^{\bullet-} + HCO_2^- \rightarrow SO_4^{2-} + CO_2^{\bullet-} + H^+ \qquad (1b)$$

In the gas-phase chemistry, a solitary $CO_2$ does not capture an excess electron as long as it retains the linear equilibrium geometry. Although $CO_2^{\bullet-}$ can be prepared via precursors containing a bent O═C═O configuration,[9] the lifetime of $CO_2^{\bullet-}$ against autodetachment is less than 100 $\mu$s.[10,11] Now considering the fact that (i) negatively charged clusters of carbon dioxide, $(CO_2)_N^-$, are readily formed in the collisions of neutral $(CO_2)_M$ clusters with slow electrons,[12−18] high-Rydberg atoms,[19−22] or alkali atom[23] and that (ii) the lifetimes of the resultant $(CO_2)_N^-$ are estimated to be at least 2 ms,[12] one might reach the possibility of utilizing the $(CO_2)_M + e^-$ system for the reductive activation of $CO_2$.

In our previous study, we investigated the reactions of $(CO_2)_N^-$ with alkyl iodides, such as $CH_3I$, $C_2H_5I$, and 2-$C_3H_7I$.[24]

**SCHEME 1**

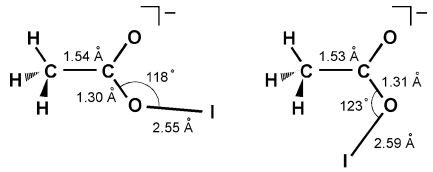


**1** **2**

We have found that $(CO_2)_N^-$ with $N \leq 6$ react with $CH_3I$ to form an acetyloxy iodide anion, $CH_3CO_2I^-$ (Scheme 1[25]):

$$(CO_2)_N^- + CH_3I \rightarrow CH_3CO_2I^-(CO_2)_n + (N - n - 1)CO_2, \quad n = 0, 1, 2 \qquad (2)$$

Ab initio calculations showed that in $CH_3CO_2I^-$ the acetyloxyl framework binds the I atom through an O−I bond; the molecular orbital arising mainly from the *p* orbitals of I and the adjacent O atom accommodates the excess electron.[26] It was also found that the reaction is strongly subject to steric hindrance around the carbon site of alkyl iodides. In fact, the reaction of $(CO_2)_N^-$ with 2-$C_3H_7I$ was found to yield no product anions of the formula 2-$C_3H_7CO_2I^-$. This suggests that $CH_3CO_2I^-$ is formed via a transition state prepared by a nucleophilic attack of $(CO_2)_N^-$ on the carbon site of alkyl iodide,[24] while the first look at the final product $CH_3CO_2I^-$ suggests insertion of $CO_2^{\bullet-}$ between the C−I bond of $CH_3I$. Although there still remains much room for discussion regarding the formation mechanism of $CH_3CO_2I^-$, the previous $(CO_2)_N^-$ + $CH_3I$ study has shown for the first time that $(CO_2)_N^-$ serve as a neucleophile in the gas-phase reactions.

As for the geometrical and electronic structures of $(CO_2)_N^-$, several investigations have been made both theoretically[27−30] and experimentally.[31−33] Recent photoelectron spectroscopic studies have revealed, in consonance with the theoretical predictions,[27,29] that $C_2O_4^-$ is formed as the anionic core of $(CO_2)_N^-$ in the size range $2 \leq N \leq 5$ and $N \geq 14$, whereas the

* Corresponding author. E-mail: nagata@cluster.c.u-tokyo.ac.jp.
† Institute for Molecular Science.
‡ The University of Tokyo.

10.1021/jp0350767 CCC: $25.00 
Published on Web 09/16/2003

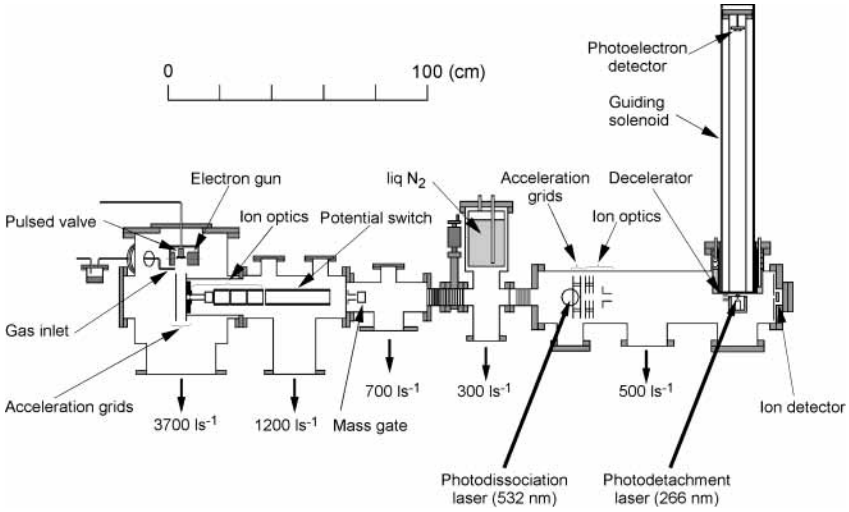


**Figure 1.** Schematic of the experimental apparatus.

excess electron is localized on a $CO_2$ moiety for $7 \leq N \leq 12$.[32,33] The two forms of "electronic isomers", $C_2O_4^-(CO_2)_{N-2}$ and $CO_2^{\bullet-}(CO_2)_{N-1}$, coexist at $N = 6$ and 13. It was also reveled from photoelectron-depletion experiment that the $(CO_2)_6^-$ cluster fluctuates between the two isomeric forms at the beam temperature: $C_2O_4^-(CO_2)_4 \leftrightarrow CO_2^{\bullet-}(CO_2)_5$.[33] As only one $CO_2$ remains in the framework of $CH_3CO_2I^-$ produced in the $(CO_2)_N^- + CH_3I$ reaction, $C_2O_4^- \rightarrow CO_2^{\bullet-}$ transformation takes place inevitably during the formation of a collision complex between $(CO_2)_N^-$ ($N \leq 6$) and $CH_3I$.[24] Now a naive question arises regarding the structural properties of $(CO_2)_N^-$ relevant to the reactivity: namely, whether the $C_2O_4^-(CO_2)_{N-2}$ structure is essential to the formation of $CH_3CO_2I^-$ in the $(CO_2)_N^- + CH_3I$ reaction.

In the present study, we have examined the product anions in the gas-phase reaction of $CO_2^{\bullet-}(H_2O)_N$ with $CH_3I$ by using conventional mass spectrometry combined with a photofragmentation experiment. The use of $CO_2^{\bullet-}(H_2O)_N$ as the reagent provides us with the following advantages:

(1) Owing to the negative electron affinity of $CO_2$ and short lifetime of $CO_2^{\bullet-}$, it is difficult to prepare a beam of $CO_2^{\bullet-}$ anion radicals with an intensity sufficient not merely for detection but for reaction experiments. By contrast, $CO_2^{\bullet-}(H_2O)_N$ are easily prepared through electron attachment to neutral $(CO_2)_K(H_2O)_L$ clusters in an electron-impact ionized free jet. The hydration also tends to stabilize $CO_2^{\bullet-}$ by increasing the potential barrier height against autodetachment.[28]

(2) As $CO_2^{\bullet-}(H_2O)_N$ contains only monomer $CO_2^{\bullet-}$, the $CO_2^{\bullet-}(H_2O)_N + CH_3I$ study gives us a direct answer to the above question regarding the reactive species responsible for the $CH_3CO_2I^-$ formation. When the $CO_2^{\bullet-}(H_2O)_N + CH_3I$ reaction is found to result in the formation of $CH_3CO_2I^-$, we are ready to adopt a reaction mechanism where $C_2O_4^-$ is transformed swiftly into $CO_2^{\bullet-}$ in the early stage of the $(CO_2)_N^- + CH_3I$ reaction.

(3) The $CO_2^{\bullet-}$ anion radical represents a class of reagents in which the radical and charge sites are spatially separated.[34] Ab initio calculations show that the unpaired electron is residing primarily on the C atom with a spin density of $\approx$0.88, while the excess charge is localized on the O atoms with the Mulliken charge distribution of $\approx -0.69$ for each (see section 3C). Therefore, in $CO_2^{\bullet-}(H_2O)_N$, hydration is expected to occur with the solvent $H_2O$ molecules interacting with the O atoms of $CO_2^{\bullet-}$ through O$\cdots$H$-$O linkages. This probably results in the retardation of reactions involving charge-transfer processes, as is the case in bimolecular nucleophoilic substitution ($S_N2$) reactions between anions and polar molecules, and consequently elicits the reactivities of $CO_2^{\bullet-}(H_2O)_N$ characteristic of open-shell radicals.

The purpose of the present study is (i) to demonstrate a possible way for reductive activation of otherwise inert $CO_2$ by exploiting the positive electron affinity of gas-phase clusters and (ii) to unveil the reactivity intrinsic to $CO_2^{\bullet-}$ sustained in the clusters. From this point of view, we first discuss in this article the chemical identity of the reagents $[(CO_2)(H_2O)_N]^-$ prepared in our ion beam, based on the measured photoelectron spectra, and confirm the selective preparation of hydrated $CO_2^{\bullet-}$ anion radicals, $CO_2^{\bullet-}(H_2O)_N$, under the present experimental conditions. The product anions in the $CO_2^{\bullet-}(H_2O)_N + CH_3I$ reaction are then identified by combining product mass analysis with photofragmentation analysis of the anions of interest. By comparing the experimental results with those in the $(CO_2)_N^- + CH_3I$ study, the reaction mechanism operative in the $CO_2^{\bullet-}(H_2O)_N + CH_3I$ system is discussed with the aid of ab initio calculations on the structural properties of hydrated $CO_2^{\bullet-}$ anion radicals.

## Experimental Section

Figure 1 shows the schematic of the experimental setup.[24] The apparatus consists of a cluster anion source, a tandem time-of-flight (TOF) mass spectrometer, and a photoelectron spectrometer. The $[(CO_2)(H_2O)_N]^-$ reactants are prepared by electron attachment to neutral $(CO_2)_K(H_2O)_L$ clusters in an electron-impact ionized free jet.[35] The $(CO_2)_K(H_2O)_L$ clusters are formed by pulsed expansion of 1-atm of $CO_2$ gas containing a trace amount of $H_2O$. An injection of 250-eV electrons into the expansion region results in the production of secondary slow electrons, which are trapped efficiently by $(CO_2)_K(H_2O)_L$ to form $[(CO_2)_M(H_2O)_N]^-$:

$$(CO_2)_K(H_2O)_L + e^- \text{ (slow)} \rightarrow [(CO_2)_M(H_2O)_N]^- + (K-M)CO_2 + (L-N)H_2O \quad (3)$$

At a certain gas mixture condition, the only anionic species produced in the ionized beam are $[(CO_2)(H_2O)_N]^-$ clusters. The $[(CO_2)(H_2O)_N]^-$ anions are then extracted at $\approx$15 cm downstream from the nozzle, perpendicularly to the initial beam direction, by applying a pulsed electric field of 20 V cm$^{-1}$. The

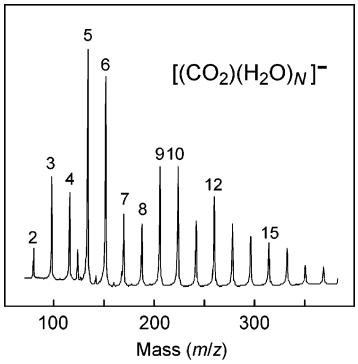


**Figure 2.** Mass spectrum of $[(CO_2)(H_2O)_N]^-$ prepared in the electron-impact ionized free jet of $CO_2$ containing a trace amount of $H_2O$. The number at each peak represents the number, $N$, of $H_2O$ molecules in $[(CO_2)(H_2O)_N]^-$.

anions are further accelerated up to 500 eV, mass-analyzed by a 2.3-m TOF mass spectrometer, and detected by a microchannel plate (Hamamatsu MCP F4655-10). The resolution of the TOF mass spectrometer is $m/\Delta m \approx 500$. The signals from the MCP are amplified and accumulated by a 500-MHz digitizing oscilloscope (Tektronix TDS520A). A typical mass spectrum of $[(CO_2)(H_2O)_N]^-$ thus obtained is shown in Figure 2.

The $CH_3I$ target sample (Kanto Chemicals, >98% purity) is introduced into the source chamber through an effusive nozzle. The pressure of the chamber increases from $\approx 1 \times 10^{-7}$ to $\approx 2 \times 10^{-5}$ Torr when the $CO_2$ jet is on and up to $\approx 1 \times 10^{-4}$ Torr with the introduction of $CH_3I$ gas. The $CH_3I$ molecules in the ambient pressure are entrained into the free jet, where they encounter $[(CO_2)(H_2O)_N]^-$ clusters, while the jet is drifting in the source chamber. Side reactions, which might occur in the free jet, will be discussed in the next section. The product anions formed in the $[(CO_2)(H_2O)_N]^- + CH_3I$ reaction are extracted, mass analyzed, and detected by the same method as above.

Photoelectron measurements were performed by a magnetic bottle type photoelectron spectrometer equipped at the end of the TOF tube. Mass selection is achieved by a pulsed beam deflector (mass gate) prior to photodetachment. The ambient pressure of the photoelectron chamber is kept at $\approx 3 \times 10^{-10}$ Torr under typical operation conditions. At the photodetachment region, an unfocused fourth harmonics (266 nm) of a Q-switched Nd:YAG laser is timed to intersect the mass-selected ion bunch. The laser fluence is kept below 5 mJ pulse$^{-1}$ cm$^{-2}$. The electrons are detached in a strong inhomogeneous magnetic field ($\approx$1000 G) and further guided by a weak field ($\approx$10 G) down to a detector installed at the end of a 1-m flight tube. The photoelectrons are detected by a microsphere plate with a 27-mm diameter (El-Mul Z033DA) and counted by a multichannel scaler/averager (Stanford Research SR430). Each spectrum presented in this paper represents an accumulation of 25 000−50 000 laser shots with background subtraction. The measured electron kinetic energy is calibrated against the known photoelectron band of $I^-$ and $I^-(CO_2)$ anions.[36] The energy resolution of the spectrometer is $\approx$100 meV at the electron kinetic energy of 1 eV.

In the photodissociation measurement, the apparatus is used as a collinear tandem TOF spectrometer. The cluster anions of interest are spatially and temporally focused at the point 1.54-m downstream from the first acceleration grids. At the focus the anions are crossed with the second harmonics (532 nm) of a Q-switched Nd:YAG laser. The laser fluence used is in the range 60−70 mJ pulse$^{-1}$ cm$^{-2}$. The photofragments are then re-accelerated by a pulsed electric field (1 kV, 700-ns duration) at the second acceleration assembly. The 0.8-m flight path to the MCP detector serves as the second mass analyzer. The photofragment signals are accumulated by the digitizing oscilloscope typically for 100−1000 laser shots.

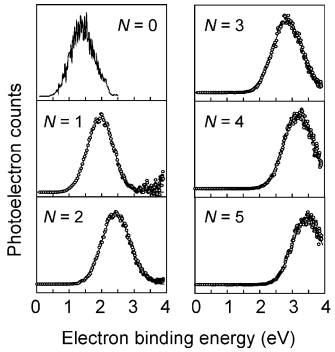


**Figure 3.** Photoelectron spectra of $[(CO_2)(H_2O)_N]^-$ with $1 \le N \le 5$ measured at the photon energy of 4.66 eV. Open circles represent the experimental data. Best-fit profiles by assuming a Gaussian function (eq 4) are shown by solid lines. The $N = 0$ spectrum is taken from ref 31.

**TABLE 1: Vertical Detachment Energies and fwhm Values Determined from the $[(CO_2)(H_2O)_N]^-$ Photoelectron Bands**

| N | VDE,[a] eV | fwhm,[b] eV |
|---|---|---|
| 1 | 1.96 | 0.94 |
| 2 | 2.44 | 1.03 |
| 3 | 2.85 | 1.08 |
| 4 | 3.21 | 1.09 |
| 5 | 3.46 | 1.09 |

[a] Experimental error is estimated to be $\approx$0.02 eV in each VDE value. [b] Experimental error is estimated to be <0.04 eV in each fwhm value.

## Results and Discussion

**A. Chemical Identity of $[(CO_2)(H_2O)_N]^-$ Reactant.** The electronic structures of the $[(CO_2)(H_2O)_N]^-$ reactants were probed by photoelectron spectroscopy. Figure 3 displays the photoelectron spectra of $[(CO_2)(H_2O)_N]^-$ with $1 \le N \le 5$ recorded at a photon energy of 4.66 eV. All the spectra observed consist of a structureless single broad peak. The spectrum of $CO_2^{\bullet -}$ monomer reported by Bowen and co-workers[31] is also shown for comparison. In these spectra, the photoelectron counts are plotted as a function of the electron binding energy defined as $E_b = h\nu - E_k$, where $h\nu$ and $E_k$ represent the photon energy and the kinetic energy of the photoelectrons, respectively. The maxima of the photoelectron bands are interpreted as vertical detachment energies (VDEs) of the cluster anions. To determine the VDE and fwhm values, the spectral profiles are fitted to a Gaussian function by a nonlinear least-squares method, where the band contour is expressed as

$$I(E_b) = C \exp[-(E_b - E_0)^2/\delta^2] \qquad (4)$$

In eq 4, $E_0$ corresponds to VDE and $\delta$ is related to the spectral width by fwhm $= 2(\ln 2)^{1/2}\delta$. The analysis revealed that the $[(CO_2)(H_2O)_N]^-$ photoelectron bands are well represented by a Gaussian function given by eq 4, as shown by solid lines in Figure 3. The VDE and fwhm values thus determined for $[(CO_2)(H_2O)_N]^-$ are listed in Table 1. The VDE value for $N = 1$ is determined to be $1.96 \pm 0.02$ eV, which is larger than that of the $CO_2^{\bullet -}$ monomer by $\approx$0.6 eV. As discussed in our previous study,[37] the observed shift of VDE is comparable to a typical value expected for an ion−dipole interaction. Hence, it

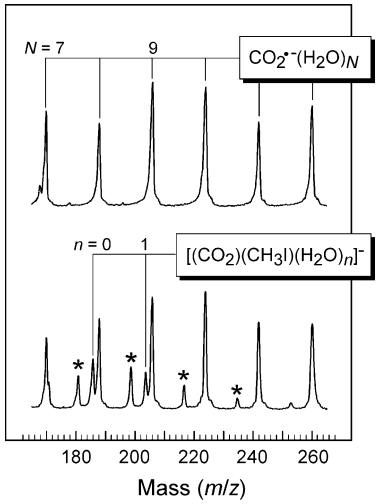


**Figure 4.** Mass spectra of the $CO_2^{\bullet-}(H_2O)_N$ reactants (upper trace) and the product anions in the reaction of $CO_2^{\bullet-}(H_2O)_N$ with $CH_3I$ (lower trace). The product mass peaks are interspersed between the unreacted $CO_2^{\bullet-}(H_2O)_N$ peaks. The peaks marked with asterisks are assignable to the family of $I^-(H_2O)_N$ ($N = 3-7$).

can be inferred that $[(CO_2)(H_2O)]^-$ possesses the electronic structure represented as $CO_2^{\bullet-}(H_2O)$, where the excess charge is localized on the $CO_2$ moiety. From $N = 1-5$, the VDE value increases by 0.25−0.3 eV with the addition of another $H_2O$ molecule. The increment in VDE with each additional $H_2O$ molecule is ascribable to the stabilization by hydration. We conclude from these results that $CO_2^{\bullet-}$ plays the role of an anionic core in $[(CO_2)(H_2O)_N]^-$ with $1 \le N \le 5$: the $[(CO_2)(H_2O)_N]^-$ species can be regarded as hydrated $CO_2^{\bullet-}$ anion radicals, $CO_2^{\bullet-}(H_2O)_N$.

As for the larger members of $[(CO_2)(H_2O)_N]^-$ with $N \ge 6$, no information on the electronic structures was obtained in the photoelectron measurements because VDEs of the larger analogues are located in the higher energy region inaccessible in the present study. We infer that $CO_2^{\bullet-}$ is formed also in the larger $[(CO_2)(H_2O)_N]^-$ ($N \ge 6$) with the following arguments. Since $(H_2O)_N^-$ with $N \le 11$ are unstable against autodetachment and/or dissociation,[38] it is unlikely that $[(CO_2)(H_2O)_N]^-$ with $6 \le N \le 11$ possess $CO_2\cdots(H_2O)_N^-$ structures. Posey et al. have reported that reaction of $(H_2O)_N^-$ ($N \ge 15$) with $CO_2$ results in the formation of $CO_2^{\bullet-}(H_2O)_{N-3}$.[39] The reaction is described by electron transfer from $(H_2O)_N^-$ to $CO_2$ followed by hydration of the resultant $CO_2^{\bullet-}$ and subsequent evaporative loss of, on the average, three $H_2O$ solvents. This indicates the preferential occurrence of the $CO_2^{\bullet-}(H_2O)_N$ structure rather than $CO_2\cdots(H_2O)_N^-$ in the size range $N \ge 12$. The present observation that only anionic species containing one $CO_2$ molecule are selectively prepared in our ionized free jet also reinforces our argument for the $CO_2^{\bullet-}(H_2O)_N$ structure of larger $[(CO_2)(H_2O)_N]^-$ reactants.

**B. Product Anions in the $CO_2^{\bullet-}(H_2O)_N + CH_3I$ Reaction.** The upper trace of Figure 4 shows a part of the mass spectrum of $CO_2^{\bullet-}(H_2O)_N$ reactants. When the $CH_3I$ reagent is introduced into the source chamber, mass peaks ascribable to the product anions emerge in the spectrum, as shown in the lower trace of Figure 4. In addition to the unreacted $CO_2^{\bullet-}(H_2O)_N$, anions with the formulas $[(CO_2)(CH_3I)(H_2O)_n]^-$ ($n = 0$ and 1) and $[I(H_2O)_n]^-$ ($3 \le n \le 7$) are detected in the mass region $160 \le m/z \le 260$. In the present experimental setup, two types of reaction pathways are possible as the $CH_3I$ sample is introduced directly into the source chamber:

$$(CO_2)_K(H_2O)_L \xrightarrow{e^-} CO_2^{\bullet-}(H_2O)_N \xrightarrow{CH_3I} \text{product anions} \quad (5a)$$

and

$$(CO_2)_K(H_2O)_L \xrightarrow{CH_3I} (CO_2)_M(H_2O)_N(CH_3I) \xrightarrow{e^-} \text{product anions} \quad (5b)$$

It was found in our previous study[24] that electron attachment to neutral $(CO_2)_M(CH_3I)_N$ clusters results exclusively in the production of $I^-(CO_2)_n$, indicating a preferential electron capture by $CH_3I$, which dissociates rapidly into $CH_3^\bullet + I^-$, in $(CO_2)_M(CH_3I)_N$. This is probably the case also in the electron attachment to $(CO_2)_M(H_2O)_N(CH_3I)$ species. Therefore, we infer that the product anions $[(CO_2)(CH_3I)(H_2O)_n]^-$ ($n = 0$ and 1) are formed primarily via pathway 5a, where preexisting $CO_2^{\bullet-}(H_2O)_N$ clusters in the ionized free jet react with ambient $CH_3I$ gas:

$$CO_2^{\bullet-}(H_2O)_N + CH_3I \rightarrow [(CO_2)(CH_3I)]^- + NH_2O \quad (6a)$$

or

$$CO_2^{\bullet-}(H_2O)_N + CH_3I \rightarrow [(CO_2)(CH_3I)(H_2O)]^- + (N-1)H_2O \quad (6b)$$

As to the formation of $I^-(H_2O)_n$, we cannot rule out the possible contribution from process 5b. Hereafter, we focus our attention on processes 6, because product anions formed via the possible charge-transfer process,

$$CO_2^{\bullet-}(H_2O)_N + CH_3I \rightarrow I^-(H_2O)_n + CH_3^\bullet + CO_2 + (N-n)H_2O \quad (7)$$

are indistinguishable from those formed via process 5b and because formation of $I^-(H_2O)_n$ is rather trivial.

Taking account of the fact that the product anion with $[(CO_2)(CH_3I)]^-$ stoichiometry has been identified as an acetyloxy iodide anion, $CH_3CO_2I^-$, in the $(CO_2)_N^- + CH_3I$ reaction,[24] it seems natural to consider the $[(CO_2)(CH_3I)]^-$ product in processes 6 as a $CH_3CO_2I^-$ anion. To confirm this argument, photofragmentaion study of the product anions was performed. In our previous study we have observed two competing fragmentation channels of $CH_3CO_2I^-$ in 532 nm photodissociation:[24,26]

$$CH_3CO_2I^- + h\nu\ (532\ nm) \rightarrow CH_3CO_2^- + I \quad (8a)$$

$$\rightarrow CH_3CO_2 + I^- \quad (8b)$$

Simultaneous occurrence of processes 8a and 8b is ascribable intrinsically to the electronic properties of $CH_3CO_2I^-$, where the excess electron is shared between the O and I atoms by occupying a molecular orbital constructed of 12a′, 13a′ orbitals of acetate and 5*p* orbital of I atom.[26] In general, photodetachment is the dominant photodestruction channel of molecular anions, either because the lowest excited state of anions is usually located higher than the vertical detachment energy or because the bond dissociation energy is larger than the threshold for electron detachment. In the case of $CH_3CO_2I^-$, however, the O−I bond dissociation energy is estimated to be ≈0.73 eV,[24] which is much smaller than the VDE of $CH_3CO_2I^-$ (3.53 ± 0.02 eV[24]). The electronic transition responsible for the 532-nm photoabsorption corresponds to the electron promotion from

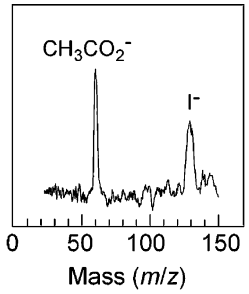


**Figure 5.** Photofragment mass spectrum resulting from the 532-nm photodissociation of $[(CO_2)_2CH_3I]^-$. Broadness of the $I^-$ peak comes from the deteriorating mass resolution in the higher mass region.

nonbonding to antibonding orbitals relevant to the O−I bond.[26] Figure 5 shows a 532-nm photofragment mass spectrum of $[(CO_2)(CH_3I)]^-$ formed in process 6a. The spectrum displays two peaks at $m/z = 59$ and 127, which are assigned to $CH_3CO_2^-$ and $I^-$, respectively. Because the appearance of both the $CH_3CO_2^-$ and $I^-$ fragments in the 532-nm photodissociation provides decisive evidence of the $[(CO_2)(CH_3I)]^-$ species being $CH_3CO_2I^-$, we conclude here that $CO_2^{\bullet-}(H_2O)_N$ reacts with $CH_3I$ to form an acetyloxy iodide anion, $CH_3CO_2I^-$. This argument allows us to say further that it is not $C_2O_4^-$ but $CO_2^{\bullet-}$ that is responsible for the formation of $CH_3CO_2I^-$ in the $(CO_2)_N^-$ + $CH_3I$ reaction. Hence, process 2 can be rewritten in detail as

$$C_2O_4^-(CO_2)_{N-2} + CH_3I \rightarrow [C_2O_4^-(CO_2)_{N-2}(CH_3I)]^\dagger \quad (9a)$$

$$[C_2O_4^-(CO_2)_{N-2}(CH_3I)]^\dagger \rightarrow [CO_2^{\bullet-}\cdots CH_3I(CO_2)_{N-1}]^\ddagger \quad (9b)$$

$$[CO_2^{\bullet-}\cdots CH_3I(CO_2)_{N-1}]^\ddagger \rightarrow CH_3CO_2I^-(CO_2)_n + (N-n-1)CO_2 \quad (9c)$$

where the $C_2O_4^- \rightarrow CO_2^{\bullet-}$ transformation (process 9b) occurs prior to the chemical reaction.

**C. Reaction Mechanism.** As discussed in the previous section, $CO_2^{\bullet-}(H_2O)_N$ acts as a gas-phase carboxylation reagent for $CH_3I$. It is difficult, however, to define the cluster size $N$ of $CO_2^{\bullet-}(H_2O)_N$ responsible for the $CH_3CO_2I^-$ formation since $CO_2^{\bullet-}(H_2O)_N$ reagents are not mass selected in the present study. To further the discussion of this point, let us first consider the energetics of process 6a. The formation process of $CH_3CO_2I^-$ from $CO_2^{\bullet-}$ + $CH_3I$ is exothermic, where the heat of reaction is given by

$$\Delta H = EA(CO_2) + D(H_3C-I) - D(H_3C-CO_2) - EA(I) - D(CH_3CO_2-I^-) \quad (10)$$

In eq 10, *EA* and *D* represent electron affinity and bond dissociation energy, respectively. By using reported values of *EA* and *D* ($EA(CO_2) = -0.60$ eV,[11] $EA(I) = 3.06$ eV,[40] $D(H_3C-I) = 2.47$ eV,[41] $D(H_3C-CO_2) = -0.33$ eV,[42] and $D(CH_3CO_2-I^-) \approx 0.73$ eV[24]), the heat of reaction is calculated to be $\Delta H \approx -1.59$ eV. As the $CO_2^{\bullet-}$ reactant is hydrated by $N$ molecules of $H_2O$ in process 6a, the exothermicity of ≈1.59 eV is transformed mainly to the evaporation energy of the solvent $H_2O$ molecules. As the O−I bond dissociation energy of $CH_3CO_2I^-$ (≈0.73 eV) is much smaller than the exothermicity (≈1.59 eV), the rapid energy dissipation as the evaporation energy of $H_2O$ is essential to the stabilization of otherwise dissociating product $CH_3CO_2I^-$. The collision energy incorporated into the total energy of reaction is negligibly small because very low-energy collision conditions are achieved in our experimental setup, where the target molecules are entrained into the stream of the ionized jet drifting in the $CH_3I$ environment. Assuming that the binding energy of a $H_2O$ solvent onto the $CO_2^{\bullet-}$ core is ≈0.7 eV (see below), a maximum of two or three $H_2O$ solvents are lost in processes 6. This means that small members of $CO_2^{\bullet-}(H_2O)_N$ with $N \approx 2-4$ primarily contribute to the formation of $CH_3CO_2I^-$. We should refer to another possibility that the overall reaction proceeds as

$$CO_2^{\bullet-}(H_2O)_N + CH_3I \rightarrow CH_3CO_2I^- + (H_2O)_M + (N-M)H_2O \quad (11)$$

where neutral water clusters are formed eventually through the rupture of hydrogen bonds between the $CO_2^{\bullet-}$ core and $(H_2O)_N$ moiety. In this case, larger $CO_2^{\bullet-}(H_2O)_N$ species might come into the reaction since less energy is required for the solvent evaporation. We will discuss the possibility of process 11 later in this section.

It is interesting and even more informative to compare the present reaction system with gas-phase nucleophilic displacement ($S_N2$) reactions in terms of microsolvation effects on the reaction rate. There have been a number of theoretical and experimental studies on the solvent effect on $S_N2$ reactions of the type

$$X^-S_m + RY \rightarrow [X\cdots R\cdots Y]^-S_m \rightarrow Y^-S_n + RX + (m-n)S \quad (12)$$

where $X^-$, S, and Y represent a negatively charged nucleophilic reagent, a solvent molecule, and a leaving group having a positive electron affinity, respectively.[43] Those studies have revealed that hydration reduces the reactivity of nucleophilic reagents significantly, being consistent with the gas-phase $S_N2$ model proposed by Olmstead and Braumann:[44] the reduction of reactivity by hydration arises from a higher barrier due to the more effective solvation of the charge-localized reactant, $X^-$, relative to the charge-delocalized transition state, $[X\cdots R\cdots Y]^-$. For example, the displacement pathway is quenched almost completely in the $OD^-(D_2O)_3 + CH_3Br$ reaction.[45] In the case of $Cl^-(D_2O)_n + CH_3Br$, solvent exchange to form $Cl^-(CH_3Br)(D_2O)_m$ was found to be the dominant process for $n = 1-3$.[46] On the contrary, hydration does not primarily retard the reactions of $CO_2^{\bullet-}$ with $CH_3I$ in the present study. This difference in the hydration effect suggests that the $S_N2$ mechanism involving a $[X\cdots R\cdots Y]^-S_m$ type of transient does not operate in the $CO_2^{\bullet-}(H_2O)_N + CH_3I$ reaction. In our previous study, we have observed a clear effect of steric hindrance in the $(CO_2)_N^- + RI \rightarrow CH_3CO_2I^-$ (R = $CH_3$, $C_2H_5$, and 2-$C_3H_7$) reactions; the reaction is retarded to a considerable extent when the C atom of alkyl iodide is flanked by methyl groups. The same trend is also observed in qualitative measurements using $C_2H_5I$ and 2-$C_3H_7I$ in the present study. This indicates that the attack of $(CO_2)_N^-$ and/or $CO_2^{\bullet-}(H_2O)_N$ occurs on the C atom from the hindered side of alkyl iodide. Although our findings of the steric hindrance are suggestive of the operation of the $S_N2$ mechanism,[24] the observed hydration effect—or rather the absence of strong hydration effect—in the present study obviously conflicts with the reaction mechanism via the $[X\cdots R\cdots Y]^-S_m$ transition state. The actual mechanism operative in processes 6 should involve a transient species, where a large portion of the negative charge is still remaining in the $CO_2$ moiety. This argument leads us to describe the essence of the $CO_2^{\bullet-}(H_2O)_N + CH_3I$ reaction as Scheme 2, where the transient species is formed via the nucleophilic radi-

**SCHEME 2**

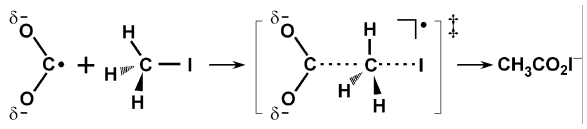


cal addition of $CO_2^{\bullet-}$. For further information on the $[^-O_2C\cdots CH_3\cdots I]^{\bullet\ddagger}$ transient and the succeeding pathway to $CH_3CO_2I^-$, rigorous ab initio studies are now awaited.

**D. Structural Properties of $CO_2^{\bullet-}(H_2O)_N$ Reactant.** To obtain information on the structural characteristics of $CO_2^{\bullet-}(H_2O)_N$ as a radical reagent, we have performed ab initio calculations. The purpose of the present calculations is to show the existence of a possible structure of $CO_2^{\bullet-}(H_2O)_N$ in which the radical point on the carbon atom of $CO_2^{\bullet-}$ is exposed outside the cluster so as to retain radical reactivity; no effort has been made to survey all the possible structures at local minima of the potential energy surface of $CO_2^{\bullet-}(H_2O)_N$ and/or the structure corresponding to the global minimum. The programs used were GAUSSIAN 98.[47] We started the geometry optimization from $N = 2$ with an initial geometry having two water molecules which interact with $CO_2^{\bullet-}$ through O−H···O bonds on the far side of the radical point. The possibility of hydration on the C atom of $CO_2^{\bullet-}$ can be ruled out based on the previous results that $H_2O$ interacts with $CO_2^{\bullet-}$ only through O−H···O linkages.[28] The initial geometry for $N = 3$ was constructed by adding another water molecule to the optimized structure for $CO_2^{\bullet-}(H_2O)_2$. The $N = 4$ initial geometry was from the $N = 3$ optimized structure, and so on. The stabilities of all the optimized structures were examined by evaluating the harmonic frequencies at the same level of approximation. For $N = 4$ TIGHT option of GAUSSIAN 98 was used to ensure the reliability of the optimization; the optimization procedures with and without TIGHT option provide an identical optimized structure for $N = 4$. Figure 6 shows the geometries of $CO_2^{\bullet-}(H_2O)_N$ with $N = 2-5$ optimized at the MP2/6-31+G* level of approximation. To save space, the structure parameters for $CO_2^{\bullet-}(H_2O)_N$ ($N = 2-5$) are given in the supporting information. In all the structures obtained in the present calculations, more than 80% of the spin density is concentrated on the carbon atom of $CO_2^{\bullet-}$, whereas the excess charge is localized mainly on the O atoms of $CO_2^{\bullet-}$ (Table 2). The hydration occurs on the O atoms of $CO_2^{\bullet-}$, due primarily to the charge localization. Thus the *ab initio* results demonstrate that $CO_2^{\bullet-}(H_2O)_N$ can take on structural forms characterizable as radical reagents. The occurrence of hydration on the O atoms is also in consonance with the modest effects of hydration on the reactivity of $CO_2^{\bullet-}(H_2O)_N$. The calculations provides the MP2 energies of $CO_2^{\bullet-}(H_2O)_N$ along with the energies required for evaporating one $H_2O$ molecule from $CO_2^{\bullet-}(H_2O)_N$, as listed in Table 3. The values estimated for the evaporation energies are in the range 0.54−0.79 eV, while the MP2 energy for the process

$$CO_2^{\bullet-}(H_2O)_4 \rightarrow CO_2^{\bullet-} + (H_2O)_4 \qquad (13)$$

is calculated to be $\Delta H = 1.31$ eV.[48] This energetic consideration suggests that process 11, the less energy-demanding channel, is favored in the reactions involving larger $CO_2^{\bullet-}(H_2O)_N$.

As for the larger $CO_2^{\bullet-}(H_2O)_N$ species, we have encountered an inevitable difficulty in performing the geometry optimization, first, because of the consumption of a huge CPU time for the MP2/6-31+G* calculations and, second, because of the existence of an increasing number of possible isomeric forms for larger $CO_2^{\bullet-}(H_2O)_N$. An attempt was made to obtain a possible hydration structure of larger $CO_2^{\bullet-}(H_2O)_N$ species by using a lower level of approximation; we chose $CO_2^{\bullet-}(H_2O)_{10}$ as an example and optimized its geometry at the UHF/6-31+G* level. During the course of geometry optimization for $N = 2-5$, we

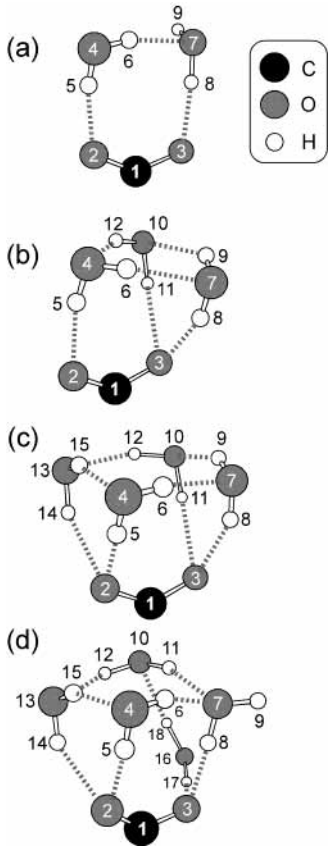


**Figure 6.** Geometries of $CO_2^{\bullet-}(H_2O)_N$ obtained by the MP2/6-31+G* calculation: (a) $CO_2^{\bullet-}(H_2O)_2$; (b) $CO_2^{\bullet-}(H_2O)_3$; (c) $CO_2^{\bullet-}(H_2O)_4$; (d) $CO_2^{\bullet-}(H_2O)_5$.

**TABLE 2: Charge and Spin Density Distributions in the $CO_2$ Moiety of $CO_2^{\bullet-}(H_2O)_N$**

| | atomic charge[a] | | | spin density[a] | | |
|---|---|---|---|---|---|---|
| N | C(1)[b] | O(2)[b] | O(3)[b] | C(1)[b] | O(2)[b] | O(3)[b] |
| 2 | 0.54 | −0.74 | −0.78 | 0.84 | 0.080 | 0.064 |
| 3 | 0.57 | −0.72 | −0.85 | 0.83 | 0.074 | 0.087 |
| 4 | 0.57 | −0.80 | −0.80 | 0.81 | 0.088 | 0.088 |
| 5 | 0.60 | −0.79 | −0.82 | 0.84 | 0.088 | 0.058 |
| $CO_2^{\bullet-}$ [c] | 0.38 | −0.69 | −0.69 | 0.88 | 0.058 | 0.058 |

[a] Mulliken charges and spin densities calculated for the optimized geometries of $CO_2^{\bullet-}(H_2O)_N$ at the MP2/6-31+G* level. [b] Numbers in parentheses correspond to the serial numbers of atoms shown in Figure 6. [c] Charge- and spin-density distributions in a bare $CO_2^{\bullet-}$ are shown for comparison.

**TABLE 3: Ab Initio Energies and Stabilization Energies of $CO_2^{\bullet-}(H_2O)_N$**

| N | energy,[a] hartree | stabilization energy,[b] eV |
|---|---|---|
| 1[c] | −264.319 86[c] | 0.63[c] |
| 2 | −340.558 52 | 0.79 |
| 3 | −416.794 95 | 0.73 |
| 4 | −493.030 91 | 0.71 |
| 5 | −569.260 49 | 0.54 |

[a] MP2 energies obtained in the geometry optimization procedures. [b] Stabilization energy is defined here as the energy required for the dissociation process, $CO_2^{\bullet-}(H_2O)_N \rightarrow CO_2^{\bullet-}(H_2O)_{N-1} + H_2O$. The energy values are calculated by using the MP2 energy of $H_2O$ (−76.209 78 hartree). [c] Taken from ref 28.

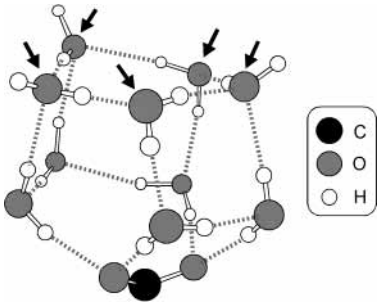


**Figure 7.** Geometry of $CO_2^{\bullet-}(H_2O)_{10}$ obtained by the UHF/6-31+G* calculation. The Mulliken spin density on the C atom of $CO_2^{\bullet-}$ is calculated to be 0.88. It should be noted that MP2 geometry optimization starting from the initial configuration prepared by removing five $H_2O$ molecules (indicated by arrows) provides the $CO_2^{\bullet-}(H_2O)_5$ structure (d) shown in Figure 6.

found that the UHF/6-31+G* calculations provide optimized geometries almost identical to those finally obtained at the MP2/6-31+G* level and that in the former calculations the distances of O···H linkages are calculated to be longer by 5−10% than those in the latter. By considering these findings, we infer that the UHF/6-31+G* calculations give a reasonable estimate for describing the motif of the hydration network constructed in $CO_2^{\bullet-}(H_2O)_{10}$, except that the relevant structure parameters are less accurate. Figure 7 depicts the geometry of $CO_2^{\bullet-}(H_2O)_{10}$ optimized by the present UHF/6-31+G*calculations. As seen in Figure 7, there exists at least one stable structure recognized as a radical reagent even in the large $CO_2^{\bullet-}(H_2O)_N$ species with $N = 10$. As is the case in $N = 4$ and 5, $CO_2^{\bullet-}$ is bound to the $(H_2O)_N$ moiety by four O$^-$H···O linkages. This is suggestive of the contribution of larger $CO_2^{\bullet-}(H_2O)_N$ to the $CH_3CO_2I^-$ formation via the energetically favorable pathway described as process 11.

## Conclusion

In summary, we report on the gas-phase reactions of hydrated $CO_2^{\bullet-}$ anion radical with $CH_3I$. The electronic properties of the reactants, $CO_2^{\bullet-}(H_2O)_N$, are probed by negative-ion photoelectron spectroscopy, which reveals the localization of the excess charge on the $CO_2$ moiety to form a $CO_2^{\bullet-}$ core in the clusters. The structural properties of the $CO_2^{\bullet-}(H_2O)_N$ reactants are examined by ab initio calculations at the MP2/6-31+G* level of theory. The product anions in the $CO_2^{\bullet-}(H_2O)_N + CH_3I$ reactions are identified by mass spectrometry combined with a photofragmentation technique. The followings are what we have found in the present study:

(1) Hydrated carbon dioxide anion radicals, $CO_2^{\bullet-}(H_2O)_N$, react with $CH_3I$ to form an acetyloxy iodide anion, $CH_3CO_2I^-$, and its hydrate. This is a sharp contrast to the reactions of $CO_2^{\bullet-}$ in the condensed phase, where the interaction of $CO_2^{\bullet-}$ with alkyl halides (RX) leads to the formation of $X^-$ through the dissociative electron capture by RX molecules.

(2) The comparison of the present results with those obtained in the previous $(CO_2)_N^-$ study[24] has revealed that $CO_2^{\bullet-}$ is responsible for the $CH_3CO_2I^-$ production in the $(CO_2)_N^- + RI$ reactions, where the $(CO_2)_N^-$ reactants take on the $C_2O_4^-(CO_2)_{N-2}$ form.

(3) Hydration does not quench efficiently the reaction pathway leading to the $CH_3CO_2I^-$ formation, being in contrast to the strong hydration effects observed in the gas-phase $S_N2$ reactions. This finding is indicative of the operation of radical-addition mechanism in the $CO_2^{\bullet-}(H_2O)_N + CH_3I$ reaction. Ab initio calculations also show that $CO_2^{\bullet-}(H_2O)_N$ can retain structural forms suitable for radical reactions: namely, the C atom of $CO_2^{\bullet-}$ carries a large spin density, which is exposed outside the clusters.

Thus, we have demonstrated unique properties of $CO_2^{\bullet-}(H_2O)_N$ as a gas-phase radical reagent. The reaction system described here can be regarded as a type of "cluster-mediated" reaction: we take advantage of the positive electron affinities of $(CO_2)_K$-$(H_2O)_L$ to prepare $CO_2^{\bullet-}(H_2O)_N$ reagents via reductive activation; the $(H_2O)_N$ moiety of the cluster reagents acts not only as a sustainer of the unstable $CO_2^{\bullet-}$ but also as a stabilizer of the resultant $CH_3CO_2I^-$.

**Acknowledgment.** We are grateful to Professor K. Takatsuka for the loan of a high-performance computer (HIT PSC-P4L), without which we could not timely complete ab initio calculations. Drs. H. Ushiyama and Y. Arasaki are also acknowledged for their technical help in the computational procedure. We thank Dr. K. Hashimoto (Tokyo Metropolitan University) for helpful discussion on the $CH_3CO_2I^-$ structures, especially for pointing out the existence of possible isomers. This work was supported in part by a Grant-in-Aid for Scientific Research from the Ministry of Education, Culture, Sports, Science and Technology under Grant No. 12440160.

**Supporting Information Available:** Structure parameters for $CO_2^{\bullet-}(H_2O)_N$ ($N = 2-5$) obtained at the MP2/6-31+G* level. This material is available free of charge via the Internet at http://pubs.acs.org.

## References and Notes

(1) Morkovnik, A. F.; Okhlobystin, O. Yu. *Usp. Khim.* **1979**, *48*, 1968.
(2) Todres, Z. V. *Organic Ion Radicals. Chemistry and Applications*; Marcel Dekker: New York, 2003.
(3) Beckwith, A. L. J.; Norman, R. O. C. *J. Chem. Soc. (B)* **1969**, 400.
(4) Edge, D. J.; Norman, R. O. C. *J. Chem. Soc. (B)* **1970**, 1083.
(5) Anderson, A. J.; Edge, D. J.; Norman, R. O. C.; West, P. R. *J. Chem. Soc. (B)* **1971**, 1004.
(6) Land, E. J.; Swallow, A. J. *Biochemistry* **1969**, *8*, 2117.
(7) Ito, T.; Hatta, H.; Nishimoto, S. *Int. J. Radiat. Biol.* **2000**, *76*, 683.
(8) Rosso, J. A.; Bertolotti S. G.; Braun, A. M.; Mártire, D. O.; Gonzalez, M. C. *J. Phys. Org. Chem.* **2001**, *14*, 300.
(9) Cooper, C. D.; Compton, R. N. *Chem. Phys. Lett.* **1972**, *14*, 29.
(10) Cooper, C. D.; Compton, R. N. *J. Chem. Phys.* **1973**, *59*, 3550.
(11) Compton, R. N.; Reinhardt,; P. W. Cooper, C. D. *J. Chem. Phys.* **1975**, *63*, 3821.
(12) Klots, C. E.; Compton, R. N. *J. Chem. Phys.* **1977**, *67*, 1779.
(13) Klots, C. E.; Compton, R. N. *J. Chem. Phys.* **1978**, *69*, 1636.
(14) Stamatovic, A.; Leiter, K.; Ritter, W.; Stephan, K.; Märk, T. D. *J. Chem. Phys.* **1985**, *83*, 2942.
(15) Knapp, M.; Kreisle, D.; Echt, O.; Sattler, K.; Recknagel, E. *Surf. Sci.* **1985**, *156*, 313.
(16) Knapp, M.; Echt, O.; Kreisle, D.; Märk, T. D.; Recknagel, E. *Chem. Phys. Lett.* **1986**, *126*, 225.
(17) Langosh, H.; Haberland, H. *Z. Phys. D* **1986**, *2*, 243.
(18) Alexander, M. L.; Johnson, M. A.; Levinger, N. E.; Lineberger, W. C. *Phys. Rev. Lett.* **1986**, *57*, 976.
(19) Kondow, T.; Mitsuke, K. *J. Chem. Phys.* **1985**, *83*, 2612.
(20) Kondow, T. *J. Phys. Chem.* **1987**, *91*, 1307.
(21) Kraft, T.; Ruf, M.-W.; Hotop, H. *Z. Phys.* **1989**, *D14*, 179.
(22) Misaizu, F.; Mitsuke, K.; Kondow, T.; Kuchitsu, K. *J. Chem. Phys.* **1991**, *94*, 243.
(23) Quitevis, E. L.; Herschbach, D. R. *J. Phys. Chem.* **1989**, *93*, 1136.
(24) Tsukuda, T.; Saeki, M.; Iwata, S.; Nagata, T. *J. Phys. Chem. A* **1997**, *101*, 5103.
(25) Although structure **1** has been reported in ref 26 as the global minimum one for $CH_3CO_2I^-$, it turns out from further calculations that there exists another stable and almost isoenergetic structure (**2**). The geometry optimization was performed at the MP2 level of theory by employing two types of basis sets: (i) LanL2DZ, in which Dunning/Huzinaga full double-$\zeta$ is used for the $CH_3CO_2$ moiety and Hay-Wadt effective core potentials (*J. Chem. Phys.* **1985**, 82, 270, 284, 299) with double-$\zeta$ for I atom and (ii) the 6-31+G(5D, 7F) basis set for the $CH_3CO_2$ moiety along with the I atom contracted basis set, 7s6p1d/[6s5p1d], constructed by Schwerdtfeger et al. (*J. Chem. Phys.* **1989**, *91*, 1762). Saeki, M. Ph.D. Dissertation, The University of Tokyo, 1998.

(26) Saeki, M.; Zhu, L.; Tsukuda, T.; Iwata, S.; Nagata, T. *Chem. Phys. Lett.* **1997**, *280*, 348.
(27) Fleischman, S. H.; Jordan, K. D. *J. Phys. Chem.* **1987**, *91*, 1300.
(28) Saeki, M.; Tsukuda, T.; Iwata, S.; Nagata, T. *J. Chem. Phys.* **1999**, *111*, 6333.
(29) Saeki, M.; Tsukuda, T.; Nagata, T. *Chem. Phys. Lett.* **2001**, *340*, 376.
(30) Saeki, M.; Tsukuda, T.; Nagata, T. *Chem. Phys. Lett.* **2001**, *348*, 461.
(31) Bowen, K. H.; Eaton, J. G. In *The Structure of Small Molecules and Ions*; Naaman, R., Vagar, Z., Eds.; Plenum Press: New York, 1987; p 147.
(32) DeLuca, M. J.; Niu, B.; Johnson, M. A. *J. Chem. Phys.* **1988**, *88*, 5857.
(33) Tsukuda, T.; Johnson, M. A.; Nagata, T. *Chem. Phys. Lett.* **1997**, *268*, 429.
(34) Schröder, D.; Schalley, C. A.; Harvey, J. N.; Schwarz, H. *Int. J. Mass Spectrom.* **1999**, *185/186/187*, 25.
(35) Johnson, M. A.; Lineberger, W. C. In *Techniques in Chemistry*; Farrar, J. M., Saunders, W. H., Eds.; Wiley: New York, 1988; Vol. 20, p 591.
(36) Arnold, D. W.; Bradforth, S. E.; Kim, E. H.; Neumark, D. M. *J. Chem. Phys.* **1995**, *102*, 3493, 3510.
(37) Tsukuda, T.; Saeki, M.; Kimura, R.; Nagata, T. *J. Chem. Phys.* **1999**, *100*, 7846.
(38) Haberland, H.; Bowen, K. H. In *Clusters of Atoms and Molecules II*; Haberland, H., Ed.; Springer-Verlag: Berlin, 1994; p 134.
(39) Posey, L. A.; DeLuca, M. J.; Campagnola, P. J.; Johnson, M. A. *J. Phys. Chem.* **1989**, *96*, 1178.
(40) Hotop, H.; Lineberger, W. C. *J. Phys. Chem. Ref. Data* **1985**, *14*, 731.
(41) *CRC Handbook of Chemistry and Physics*; Weast, R. C., Astle, M. J., Eds.; CRC Press: Boca Raton, FL, 1988−89.
(42) The bond dissociation energy $D(H_3C-CO_2)$ is estimated from the reported values of the heat of formation of $CH_3$, $CO_2$, and $CH_3CO_2$; $\Delta H(CH_3) = 1.508$ eV, $\Delta H(CO_2) = -4.078$ eV, $\Delta H(CH_3CO_2) = 2.24$ eV.
(43) Shaik, S. S.; Schlegel, H. B.; Wolfe, S. *Theoretical Aspects of Physical Organic Chemistry. The $S_N2$ Mechanism*; John Wiley: New York, 1992.
(44) Olmstead, W. N.; Brauman, J. I. *J. Am. Chem. Soc.* **1977**, *99*, 4219.
(45) Hierl, P. M.; Ahrens, A. F.; Henchman, M.; Viggiano, A. A.; Paulson, J. F. *J. Am. Chem. Soc.* **1986**, *108*, 3142.
(46) Seely, J. V.; Morris, R. A.; Viggiano, A. A.; Wang, H.; Hase, W. L. *J. Am. Chem. Soc.* **1997**, *119*, 577.
(47) Gaussian 98, Revision A.11.4, Frisch, M. J.; Trucks, G. W.; Schlegel, H. B.; Scuseria, G. E.; Robb, M. A.; Cheeseman, J. R.; Zakrzewski, V. G.; Montgomery, J. A., Jr.; Stratmann, R. E.; Burant, J. C.; Dapprich, S.; Millam, J. M.; Daniels, A. D.; Kudin, K. N.; Strain, M. C.; Farkas, O.; Tomasi, J.; Barone, V.; Cossi, M.; Cammi, R.; Mennucci, B.; Pomelli, C.; Adamo, C.; Clifford, S.; Ochterski, J.; Petersson, G. A.; Ayala, P. Y.; Cui, Q.; Morokuma, K.; Rega, N.; Salvador, P.; Dannenberg, J. J.; Malick, D. K.; Rabuck, A. D.; Raghavachari, K.; Foresman, J. B.; Cioslowski, J.; Ortiz, J. V.; Baboul, A. G.; Stefanov, B. B.; Liu, G.; Liashenko, A.; Piskorz, P.; Komaromi, I.; Gomperts, R.; Martin, R. L.; Fox, D. J.; Keith, T.; Al-Laham, M. A.; Peng, C. Y.; Nanayakkara, A.; Challacombe, M.; Gill, P. M. W.; Johnson, B.; Chen, W.; Wong, M. W.; Andres, J. L.; Gonzalez, C.; Head-Gordon, M.; Replogle, E. S.; Pople, J. A. Gaussian, Inc.: Pittsburgh, PA, 2002.
(48) The value is calculated by using the MP2 energies of $CO_2^{\bullet-}$ (−188.087 00 hartree) and $(H_2O)_4$ (−304.895 91 hartree) having a cyclic geometry. The initial configuration for the $(H_2O)_4$ geometry optimization was taken from the Cambridge Clsuter Database (Wales, D. J.; Doye, J. P. K.; Dullweber, A.; Hodges, M. P.; Naumkin F. Y.; Calvo, F.; Hernández-Rojas, J.; Middleton, T. F. http://www-wales.ch.cam.ac.uk/CCD.html; Wales, D. J.; Hodges, M. P. *Chem. Phys. Lett.* **1998**, *286*, 65).